

DOI: 10.1002/adma.200702566

## Actuating Single Wall Carbon Nanotube–Polymer Composites: Intrinsic Unimorphs\*\*

By Cheol Park,\* Jin Ho Kang, Joycelyn S. Harrison, Robert C. Costen, and Sharon E. Lowther

Electromechanical coupling effects in polymers have been routinely employed to create an array of sensors and actuators.<sup>[1–4]</sup> The most dominant coupling effects originate from piezoelectric, electrostrictive, and electrostatic (also known as the Maxwell effect) mechanisms. To generate high displacements, electrostrictive and Maxwell effects are typically exploited because the strain in such polymers is a quadratic function of the applied electric field, whereas it is linear for piezoelectrics. However, the high compliance of most electrostrictive and electrostatic polymers limits their durability and output force and reduces their applicability. Owing to their low dielectric constants relative to ceramics, polymers typically require large applied electric fields to actuate. For strain amplification, several actuator concepts have been demonstrated including multilayer and bender designs.<sup>[2,5]</sup> Most commercial actuators integrate design concepts, including unimorph, bimorph, and multimorph. These designs require extra processing steps and introduce extraneous layers such as adhesives and inactive, so-called “dummy”, layers to convert longitudinal to bending strain. The incorporation of these adhesive and inactive layers reduces the magnitude of the actuation of a given actuation system significantly and often causes delamination. Furthermore, mismatches in the thermal expansion coefficients and mechanical properties among the adhesive, inactive, and active layers can cause additional adverse effects on the actuation performance.

Here we introduce a novel electroactive single-walled carbon nanotube (SWNT)–polymer composite, an intrinsic unimorph, which can actuate to a large strain (2.6%) at relatively low driving voltages ( $<1 \text{ MV m}^{-1}$ ) while maintaining

its high performance in mechanical durability, thermal stability, and chemical resistances. This intrinsic unimorph actuator does not require adhesive or extraneous inactive layers to generate the large bending actuation. The actuating capabilities of the electroactive polymers are gained from incorporation of SWNTs into these polymers.

Actuating and sensing characteristics of composite materials are strongly dependent on their intrinsic electrical and dielectric properties, which in turn strongly rely on the SWNT dispersion in the present composite system. The well-dispersed SWNT/LaRC-EAP (Langley Research Center-ElectroActive Polyimide) composite<sup>[6,7]</sup> film was prepared by in situ polymerization under simultaneous sonication and mechanical shear based on a noncovalent interaction approach (donor–acceptor interaction between the nanotube and the polymer).<sup>[8,9]</sup> The uniform dispersion of the SWNTs (appearing as white flexible strands) throughout the polymer matrix is shown in the high-resolution scanning electron microscopy (HRSEM) image of a cryofractured cross section of a 0.5% SWNT/LaRC-EAP composite film in Figure 1A.<sup>[10]</sup> The ac conductivity of the SWNT/LaRC-EAP composites, plotted as a function of frequency on the logarithmic scale, is shown in Figure 1B. At loadings in excess of 0.05%, the composites exhibited a conductive behavior, where the conductivity is nearly independent of frequency (on the logarithmic scale). Between 0.035% and 0.05%, the conductivity increases by nine orders of magnitude. This indicates that the composite is a percolation system with a critical volume fraction ( $\phi_c$ ) between 0.035% and 0.05%.<sup>[10]</sup> This unusually low percolation was achieved by the uniform SWNT dispersion shown in Figure 1A.

The electroactive actuation of the SWNT/LaRC-EAP composite film was measured by a fiber optic sensor,<sup>[7]</sup> where out-of-plane strain ( $\epsilon_{33}$ ) was monitored in response to an applied ac electric field (0.02 Hz) through the film thickness. Figure 1C shows the strain ( $\epsilon_{33}$ ) as a function of the electric field. Displacement through the film thickness was not observed until the SWNT concentration approached the percolation threshold ( $\phi_c$ ). Just below  $\phi_c$  ( $\phi = 0.035\%$  SWNT), the composite began to displace noticeably at an applied field  $0.5 \text{ MV m}^{-1}$ . Just above  $\phi_c$  ( $\phi = 0.05\%$ ), the composite displaced significantly even at a very low applied field ( $<0.1 \text{ MV m}^{-1}$ ). Above  $\phi_c$ , the out-of-plane strain ( $\epsilon_{33}$ ) increased rapidly with increasing SWNT concentration. At concentrations above 0.2%, the composites became too conductive ( $>10^{-5} \text{ S cm}^{-1}$ ) to actuate a large strain. For the

[\*] Dr.C. Park, Dr.J. H. Kang  
National Institute of Aerospace  
MS-226, Hampton, VA 23681 (USA)  
E-mail: cheol.park-1@nasa.gov

Dr.J. S. Harrison, Dr.R. C. Costen, S. E. Lowther  
Advanced Materials and Processing Branch  
NASA Langley Research Center  
MS-226, Hampton, VA 23681 (USA)

[\*\*] We thank Z. Ounaies (Texas A&M University), P. T. Lillehei (NASA LaRC), G. Sauti (University of Witwatersrand), N. Holloway (NASA LaRC), and T.-B. Xu (National Institute of Aerospace) for their invaluable help on the experiments. J.H.K. and C.P. appreciate the NASA University Research, Engineering and Technology Institute on Bio Inspired Materials (BIMat) under award no. NCC-1-02037 for support in part. Supporting Information is available online from Wiley InterScience or from the authors.

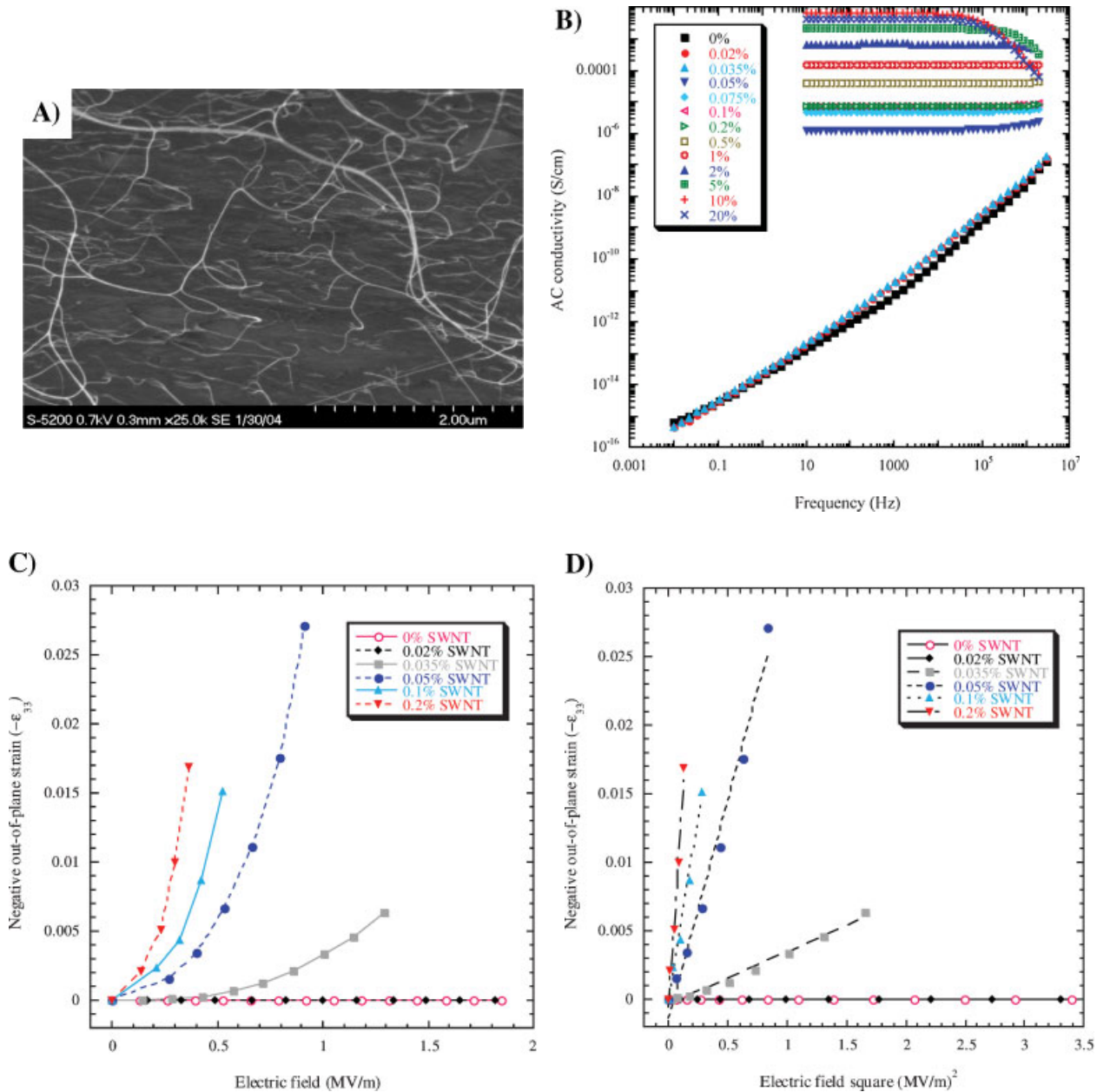


**Figure 1.** A) HRSEM of 0.5 wt % SWNT/LaRC-EAP composite (fracture surface): cross-sectional view of the composite film. B) ac conductivity of SWNT/LaRC-EAP nanocomposites as a function of frequency and SWNT concentration (percolation). C) Negative out-of-plane strain ( $-\epsilon_{33}$ ) of SWNT/LaRC-EAP composites as a function of applied electric field ( $MV m^{-1}$ ). D) Negative out-of-plane strain ( $-\epsilon_{33}$ ) of SWNT/LaRC-EAP composites as a function of the square of the applied electric field ( $MV m^{-1}$ )<sup>2</sup>.

highly conducting samples, a sufficient net field could not be applied owing to an excessive leakage current.

As shown in Figure 1C, the strain does not increase linearly with the applied field in contrast to piezoelectric materials. Rather the strain is proportional to the square of the electric field as illustrated in Figure 1D. This suggests that the actuation mechanism of the SWNT/LaRC-EAP composite is primarily due to electrostriction.<sup>[11]</sup> The strain increased as the frequency of the applied field decreased, and was observed even with a dc field. The strain response was instantaneous upon the

application of a step field application and the time to reach the saturation was found to be geometry-dependant.

A strain ( $\epsilon_{33}$ ) of 2.6% was observed for the 0.05% SWNT/LaRC-EAP composite at a field strength of only  $0.8 MV m^{-1}$ , as shown in Figure 1C and D. This strain is at least an order of magnitude greater than those of piezoelectric polymers, poly(vinylidene fluoride) (PVDF) and its copolymers (non-irradiated), and piezoceramic lead zirconate titanate (PZT). Moreover, the electric field to attain this large strain (2.6%) was only  $0.8 MV m^{-1}$ , which is an order of magnitude lower

**Table 1.** State-of-the-art electroactive materials and SWNT/LaRC-EAP[a].

Materials	Out-of-plane strain $\epsilon_{33}$ [%]	Electric field $E$ [MV m <sup>-1</sup> ]	Young's modulus $E$ [GPa]	Energy density $E\epsilon^2/2$ [J cm <sup>-3</sup> ]
PVDF [1,2]	0.1	50	1.6	0.0008
Irr-PVDF-TrFE [12,13]	5	150	0.4	0.5
Polyurethane [14,15]	11	100	0.017	0.103
PZT [3]	0.1	1	62	0.031
PZN-PT [6]	1.7	12	6.9	1.0
0.05%SWNT/LaRC-EAP	2.6	0.8	3.5	1.183

[a]Irr-PVDF-TrFE: irradiated-poly(vinylidene fluoride)-*co*-(trifluoroethylene). PZN-PT: Pb(Zn<sub>1/3</sub>Nb<sub>2/3</sub>)O<sub>3</sub>-PbTiO<sub>3</sub>.

than those required to actuate PVDF, its copolymers, and electrostrictive elastomers such as polyurethane, as shown in Table 1. This combination of flexibility, mechanical, thermal durability, and high strain at very low fields is exceptional in the realm of electroactive materials.

The comparison of the electromechanical properties displayed in Table 1 conveys the significance of the SWNT/LaRC-EAP performance. The strain energy density ( $E\epsilon^2/2$ , where  $E$  is Young's modulus) is a product of the square of the strain  $\epsilon$  and the mechanical stiffness, which is indicative of the potential mechanical work output in response to electrical stimuli. The strain energy density (1.183 J cm<sup>-3</sup>) of the SWNT/LaRC-EAP composite is at least an order of magnitude greater than any of the state-of-the-art polymeric materials reported. Its high-strain energy density is attributable to the high strain and the relatively high modulus of the LaRC-EAP polyimide. The polyimide's modulus of 3.5 GPa dwarfs that of the elastomeric materials such as polyurethane or silicone. Although the LaRC-EAP's modulus is lower than that of the brittle ceramic, PZT, its strain energy density is higher because of its higher strain. A reported ceramic PZN-PT single crystal<sup>[16]</sup> showed a comparable strain energy density (1 J cm<sup>-3</sup>) to that of SWNT/LaRC-EAP composite, however, the brittle single crystal required 12 MV m<sup>-1</sup> to produce 1.7% strain.

The field induced strain ( $\epsilon_{33}$ ) is generally represented as a power series of the applied electric field as follows:<sup>[17]</sup>

$$\epsilon_{33} = d_{33} \cdot E + M_{33} \cdot E^2 + \dots$$

where  $d_{33}$  and  $M_{33}$  are piezoelectric and electrostrictive coefficients, respectively, and  $E$  is the applied electric field. The linear and quadratic terms,  $d_{33}$  and  $M_{33}$ , respectively dominate the response. For the SWNT/LaRC-EAP, the piezoelectric contribution to the strain is not expected to be significant because the composite was not poled and has no remanent polarization. The strain caused by electrostatic (Maxwell effect), thermal, and viscoelastic effects also contributes to the quadratic coefficient. However, these effects are insignificant under the conditions of the present measurements.<sup>[18]</sup> The temperature of the film measured during actuation remained below 40 °C. For the LaRC-EAP polyimide with a glass transition temperature ( $T_g$ ) of 215 °C, this minimal heating effect precludes thermal or mechanical softening effects from contributing to the strain. The Maxwell effect can be estimated

from the equation,  $\epsilon_{\text{Maxwell}} = -s e_0 e_r E^2 (1 + 2\nu)/2$ , where  $s$  is the elastic compliance,  $e_0$  the permittivity of free space,  $e_r$  the relative permittivity, and  $\nu$  Poisson's ratio.<sup>[19]</sup> The contribution of the Maxwell effect to the strain was calculated to be less than 1% of the total strain because of the low compliance (high Young's modulus) of the polyimide matrix composites. The electrostrictive coefficients ( $M_{33}$ ) of the SWNT/LaRC-EAP composites estimated from the slopes in Figure 1D range from  $-3.8 \times 10^{-15}$  to  $-1.2 \times 10^{-13}$  m<sup>2</sup> V<sup>-2</sup>. These values are several orders of magnitude higher than those of electrostrictive polyurethanes ( $-4.6 \times 10^{-18}$  to  $-7.5 \times 10^{-17}$  m<sup>2</sup> V<sup>-2</sup>)<sup>[14,15]</sup> and irradiated-PVDF-TrFE ( $-0.37 \times 10^{-18}$  to  $-5.1 \times 10^{-18}$  m<sup>2</sup> V<sup>-2</sup>).<sup>[12,13]</sup>

In addition to out-of-plane strain, bending actuation of the SWNT/LaRC-EAP composites was demonstrated with a cantilever geometry as shown in Figure 2A and B. A video clip (Video 1, Supporting Information) shows the bending actuation of 0.05% SWNT/LaRC-EAP. Figure 2A shows the side view of the composite film without an electric field. When 0.8 MV m<sup>-1</sup> was applied, the film bent significantly, as shown in Figure 2B. A typical unimorph consists of an electroactive layer bonded to an inactive elastic layer sandwiched between electrodes.<sup>[20]</sup> The SWNT/LaRC-EAP composite film develops an "intrinsic" unimorph-type structure resulting from the film-formation process. To form a film, the composite solution is cast onto a glass substrate where it is cured. This process yields a resin-rich inactive layer and an SWNT-rich active layer. A schematic structure of the intrinsic unimorph is shown in Figure 2C. The inactive layer is formed due to a wall depletion effect during film cast on the glass substrate,<sup>[21,22]</sup> and is typically less than a few micrometers thick. When the active layer is driven to expand or contract in the plane, the inactive elastic layer resists this dimensional change, leading to bending deformation. In response to an applied electric field, the SWNT/LaRC-EAP composite contracts through the thickness and expands in the plane of the film regardless of applied field polarity. The composite film, as shown in Figure 2B, bends away from the SWNT rich active layer when a field is applied. The maximum tip displacement at a given electric field was measured for a 0.05% SWNT/LaRC-EAP film of length  $L = 40$  mm, width  $b = 5$  mm, and thickness  $h = 0.037$  mm. The tip displaced approximately 14.5 mm toward the inactive layer in response to an applied voltage of 60 V<sub>p-p</sub> (Fig. 2B). From the tip displacement ( $D_{\text{tip}}$ ), the radius of curvature ( $R$ )

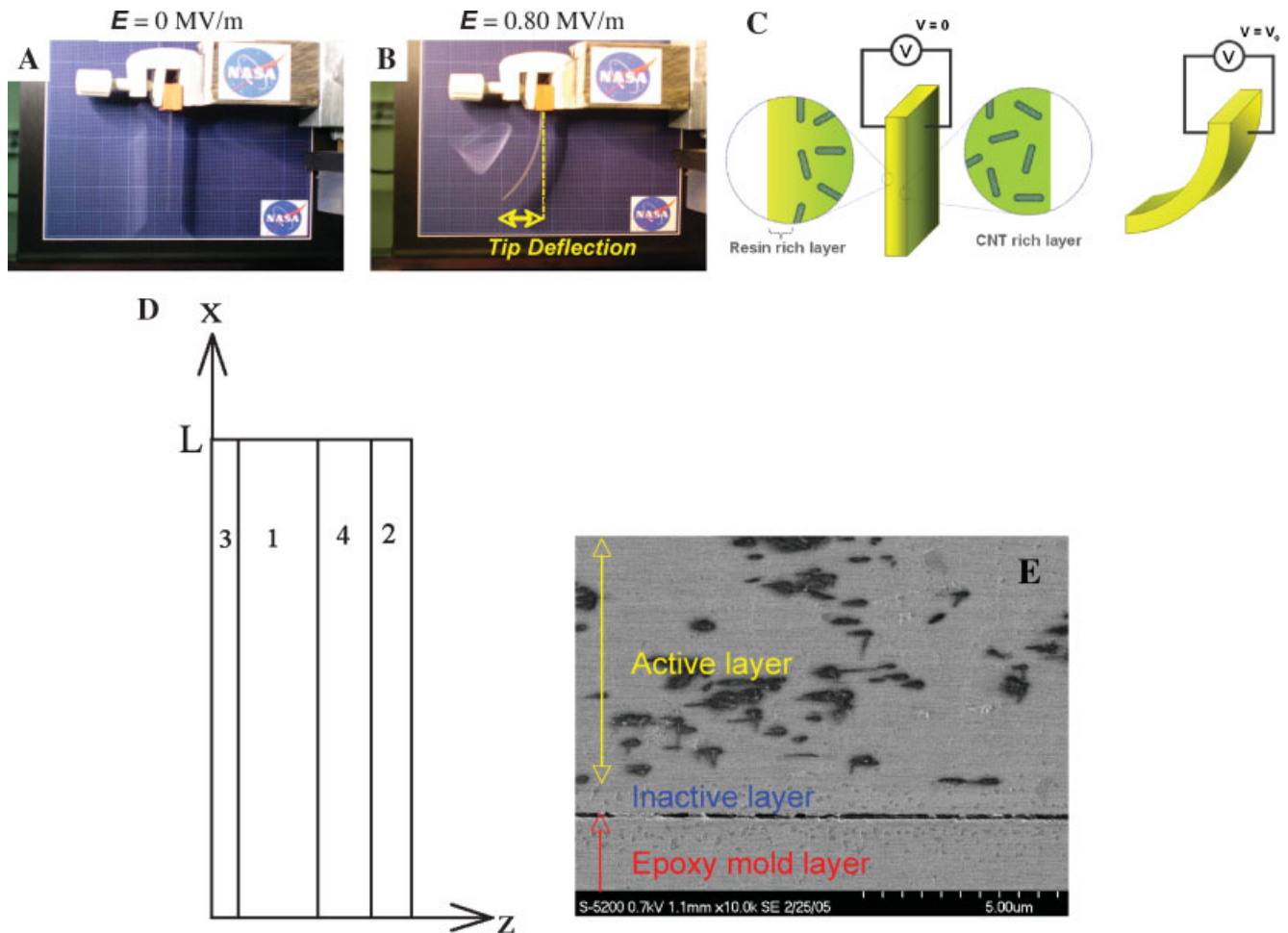


**Figure 2.** Top: Bending actuation of a cantilevered intrinsic unimorph (0.05% SWNT/LaRC-EAP) (side view): A) without, B) with an electric field (0.8 MV  $m^{-1}$ ) (see Video 1, Supporting Information), C) Schematic structure of a cross-section of the intrinsic unimorph of SWNT/LaRC-EAP composite film without and with an electric field. Bottom: D) Schematic diagram of four-layer electrostrictive bending prototype in passive state (side view). Layer widths and thicknesses are not to scale. Layer 1 is the active electrostrictive layer and layer 4 is the inactive layer. When activated, voltage  $V$  is applied between metallic layers 2 and 3. E) HRSEM micrograph of a side view of the 0.05%SWNT/LaRC-EAP composite film. The top layer is a part of the SWNT-rich active composite layer under which can be found the polymer-rich inactive layer, which lies just above the epoxy mold.

was calculated using the equation,  $D_{tip} = L^2/2R$  ( $=KL^2/2$ ,  $K$ : curvature), which gives  $R = 55.2$  mm.<sup>[23]</sup> This calculated radius of curvature from the tip displacement was very close to that measured ( $R = 53.7$  mm) experimentally (Fig. 2B).

The in-plane electrostrictive coefficient ( $M_{31}$ ) of the unimorph composite film was calculated from measurements of  $R$  and the film parameters by using a four-layer beam model.<sup>[24]</sup> A generalized schematic diagram of the prototype four-layer strip is shown in Figure 2D, where the layers are not drawn to scale. The measured input parameters for the layers are summarized in Table S1 in Supporting Information. The intrinsic unimorph formed during the process results in two layers: the electrostrictive active layer 1, and a thin inactive layer 4. Layers 2 and 3 are electrically conductive layers (silver electrodes) deposited on the outer surfaces of the electrostrictive unimorph core layers. By use of the model, the electrostrictive coefficient,  $M_{31}$  was calculated as a function of

the inactive layer thickness  $h_4$ .<sup>[24]</sup> The results are shown in Table S2 in the Supporting Information. The calculated  $M_{31}$  value ranges from  $7.5 \times 10^{-15}$  down to  $0.77 \times 10^{-15}$   $V^2 m^{-2}$  for 0.3  $\mu m$  and 3.2  $\mu m$  thick inactive layers, respectively. The measured out-of-plane electrostrictive coefficient  $M_{33}$  for this composite was  $-2.6 \times 10^{-14}$  (Fig. 1D). Assuming a Poisson's ratio ( $\nu$ ) of about 0.34, which is typical for an aromatic polyimide, the  $M_{31}$  calculated with the measured  $M_{33}$  ( $M_{31} = -M_{33} \times \nu$ ) is  $8.7 \times 10^{-15}$   $V^2 m^{-2}$ , which corresponds to an inactive layer thickness of 260 nm according to the four-layer beam model (Table S2 in Supporting Information). Figure 2E shows a scanning electron microscopy image of a cross section of a 0.05% SWNT/LaRC-EAP composite prepared by microtoming the composite film embedded in an epoxy, which reveals that the inactive layer thickness is at least thinner than 800 nm. This is consistent with the four-layer beam model results (Table S2 in Supporting Information). In

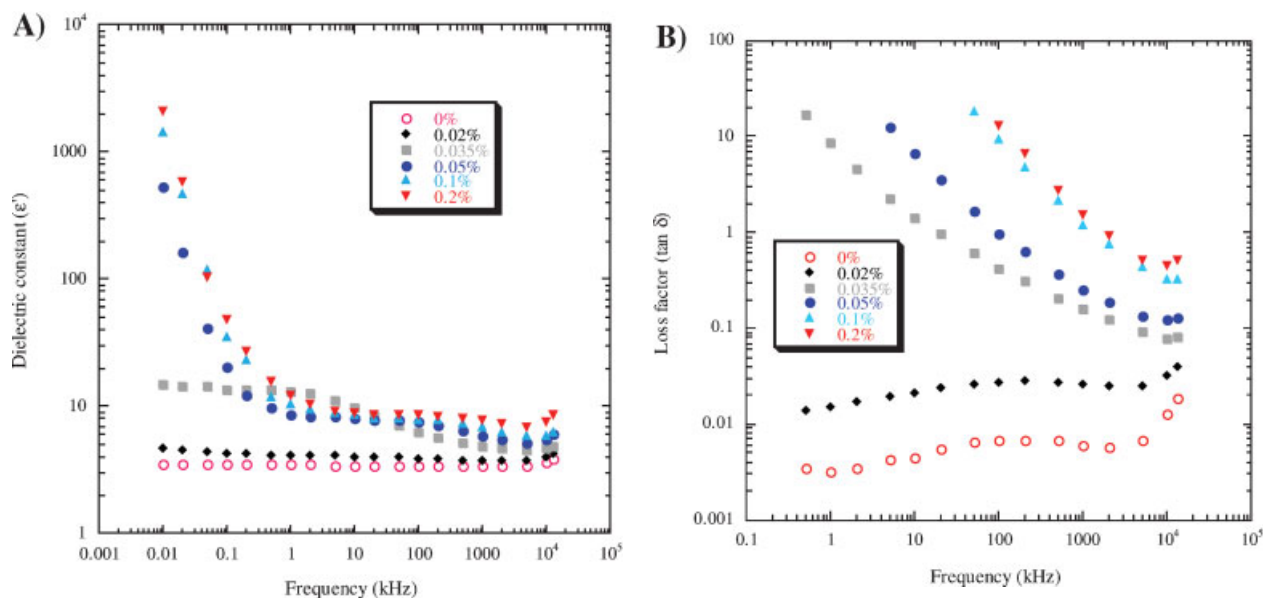


**Figure 3.** Dielectric constants of SWNT/LaRC-EAP composites as a function of the frequency, A) storage dielectric spectra, B) dielectric loss spectra.

order to ascertain the accuracy of the estimated  $M_{31}$ , it was directly measured using a dilatometer with a plastic cantilever.<sup>[25,26]</sup> The measured  $M_{31}$  was  $6.9 \times 10^{-15} \text{ V}^2 \text{ m}^{-2}$ , which is close to that estimated above.

The dielectric properties of materials are mainly determined by their polarizabilities at a given frequency. For multi-component systems, when free charge carriers migrate through the material, space charges build up at the interfaces of the constituents owing to the mismatch of the conductivities and dielectric constants of the materials at the interfaces.<sup>[27]</sup> This is called interfacial polarization. The interfacial polarization in polymers having structural inhomogeneities (e.g., nanotubes) can be identified by low-frequency dielectric measurement based on Maxwell–Wagner–Sillars’s equation.<sup>[27]</sup> This type of polarization principally influences the low-frequency ( $10^{-5}$  to  $10^2$  Hz) dielectric properties. As the frequency decreases, the time available for the drift of charge carriers increases and the observed values of dielectric constant  $\epsilon'$  become significantly higher. Also the conductivity term in interfacial polarization makes an increasing contribution to the dielectric loss as the frequency becomes smaller.

Figure 3A shows the dielectric constant of the composite films as a function of frequency and SWNT concentration as studied with an impedance analyzer. The dielectric constant of the pristine polymer at 10 Hz was around 3.5 and that of 0.02% SWNT/LaRC-EAP was 4. It increased more than three orders of magnitude between 0.035% and 0.05%, again indicating that the percolation threshold lies between these concentrations similar to the ac conductivities in Figure 1C. The increased dielectric constant of the SWNT/LaRC-EAP composites at low frequencies is likely to be caused by the interfacial polarization. The same trend, as observed for the dielectric constants, was seen in the dielectric loss spectra, which further supports the existence of interfacial polarization (Fig. 3B). This

interfacial polarization could be primarily responsible for the large strain observed in this study.<sup>[15,28]</sup> It was observed that the strain increased rapidly with decreasing frequency at low frequencies (below 1 Hz), which is consistent with the behavior of dielectric constant at low frequencies.

In summary, we developed a novel actuating SWNT/LaRC-EAP composite that exhibits a large strain (ca. 2.6%) at a low driving voltage ( $<1 \text{ MV m}^{-1}$ ) while possessing excellent mechanical and thermal properties. This composite intrinsically forms a unimorph during the fabrication process to actuate without the need for additional inactive layers. The tunable multifunctionality and structural reinforcement achieved in these composites would contribute to the design of intelligent and durable components for future aerospace vehicles as well as terrestrial applications.

## Experimental

A dilute SWNT (purified HiPco, CNI) suspension, typically around 0.05 wt %, in *N,N*-dimethylacetamide (DMAc), was prepared by sonicating for 1 h at 40 kHz. The sonicated SWNT suspension was used as a solvent for the poly(amic acid) synthesis with the diamine, 2,6-bis(3-aminophenoxy) benzonitrile (( $\beta$ -CN)APB), and the dianhydride, 4,4-oxydiphthalic anhydride (ODPA). The entire reaction was carried out with stirring in a nitrogen purged flask immersed in a 40 kHz ultrasonic bath until the solution viscosity increased and stabilized. Sonication was stopped and stirring continued for several hours to form a SWNT–poly(amic acid) solution. The solutions were cast on glass plates and cured to complete the imidization reaction to form thin SWNT–Polyimide (SWNT/LaRC-EAP) films.

The ac conductivity and the dielectric constant of the SWNT–polyimide (SWNT/LaRC-EAP) film were measured as a function of frequency with a Novocontrol–Solartron 1260 impedance/gain-phase analyzer and a HP 4192 Impedance Analyzer.

To investigate the actuating characteristics, out-of-plane displacement measurements were performed using a non-contacting fiber optic

sensor manufactured by Opto-Acoustic Sensors. Sinusoidal waveforms at a frequency of 0.02 Hz were used for all measurements. Out-of-plane polymer motion was determined by monitoring the intensity of the light reflected from the polymer surface. As the surface of the polymer film moves away from the sensor tip, the signal decreases, and as the surface moves closer to the sensor tip, the signal increases. The out-of-plane strain ( $S_{33}$ ) was measured in response to the applied electric field ( $E$ ), which is given as,  $S_{33} = \Delta t/t$ , where  $t$  is the thickness of the polymer and  $\Delta t$  is the change in thickness.

Received: October 12, 2007

Revised: December 6, 2007

Published online: May 14, 2008

- 
- [1] *Medical Applications of Piezoelectric Polymers*, (Eds: P. M. Galletti, D. E. De Rossi, A. S. De Reggi,) Gordon and Breach, New York **1988**.
- [2] *The Application of the Ferroelectric Polymers*, (Eds: T. T. Wang, J. M. Herbert, A. M. Glass,) Blackie, Chapman and Hall, New York **1988**.
- [3] A. Moulson, J. Herbert, *Electroceramics*, Chapman and Hall, London, UK **1990**, p. 293.
- [4] E. W. H. Jager, E. Smela, O. Inganäs, *Science* **2000**, *290*, 1540.
- [5] A. Dogan, J. Tressler, R. E. Newnham, *AIAA J.* **2001**, *39*, 1354.
- [6] J. O. Simpson, T. L. St. Clair, *US Patent 5891581*, **1999**.
- [7] C. Park, Z. Ounaies, K. E. Wise, J. S. Harrison, *Polymer* **2004**, *45*, 5417.
- [8] C. Park, Z. Ounaies, K. Watson, R. Crooks, J. Smith, Jr., S. E. Lowther, J. Connell, E. J. Siochi, J. S. Harrison, T. L. St. Clair, *Chem. Phys. Lett.* **2002**, *364*, 303.
- [9] K. E. Wise, C. Park, E. J. Siochi, J. S. Harrison, *Chem. Phys. Lett.* **2004**, *391*, 207.
- [10] D. S. McLachlan, C. Chiteme, C. Park, K. E. Wise, S. E. Lowther, P. T. Lillehei, E. J. Siochi, J. S. Harrison, *J. Polym. Sci. Part B* **2005**, *43*, 3273.
- [11] J. F. Nye, *Physical Properties of Crystals*, Oxford University Press, Oxford, UK **1976**.
- [12] Z.-Y. Cheng, V. Bharti, T. Mai, T.-B. Xu, Q. M. Zhang, T. Ramotowski, K. A. Wright, R. Ting, *IEEE Trans. Ultrason. Ferroelect. Freq. Control* **2000**, *47*, 1296.
- [13] C. Huang, R. Klein, F. Xia, H. Li, Q. M. Zhang, F. Bauer, Z.-Y. Cheng, *IEEE Trans. Dielectr. Electr. Insul.* **2004**, *11*, 299.
- [14] Q. M. Zhang, J. Su, C. H. Kim, R. Ting, R. Capps, *J. Appl. Phys.* **1997**, *81*, 2770.
- [15] F. M. Guillot, E. Balizer, *J. Appl. Polym. Sci.* **2003**, *89*, 399.
- [16] G. Kloops, *J. Phys. D* **1995**, *28*, 1680.
- [17] I. Krakovsky, T. Romijin, A. Posthuma de Boer, *J. Appl. Phys.* **1999**, *85*, 628.
- [18] S.-E. Park, T. Shrout, *J. Appl. Phys.* **1997**, *82*, 1804.
- [19] M. Zhenyl, J. I. Scheinbeim, J. W. Lee, B. A. Newman, *J. Polym. Sci. Part B* **1994**, *32*, 2721.
- [20] M. Watanabe, T. Hirai, M. Suzuki, Y. Amaike, *Appl. Phys. Lett.* **1999**, *74*, 2717.
- [21] L. Harnau, S. Dietrich, *Phys. Rev. E* **2002**, *65*, 021505.
- [22] P. J. A. Hartman Kok, S. G. Kazarian, B. J. Briscoe, C. J. Lawrence, *J. Colloid Interface Sci.* **2004**, *280*, 511.
- [23] M. Watanabe, H. Shirai, T. Hirai, *J. Appl. Phys.* **2001**, *90*, 6316.
- [24] F. L. Singer, *Strength of Materials*, Harper and Brothers, New York **1951**, pp 124–127.
- [25] X.-Y. Cheng, V. Bharti, T.-B. Xu, S. Wang, Q. M. Zhang, T. Ramotowski, F. Tito, R. Ting, *J. Appl. Phys.* **1999**, *86*, 2208.
- [26] For measuring the in-plane strain using the dilatometer method, the sample had one end clamped in a base vise and the other end attached to the free end of a plastic cantilever. By adjusting the height of the base vise, the sample was stretched slightly by the tension of the cantilever. Under an applied electric field, the expansion and contraction of the sample caused a deflection at the end of the cantilever detected by a fiber optic sensor. The frequency of the applied electric field was from 0.02 Hz to 3 Hz.
- [27] C. C. Ku, R. Liepins, *Electrical Properties of Polymers*, Hanserp, New York **1987**, pp. 20–58.
- [28] K. S. Suh, D. Damon, J. Tanaka, *IEEE Trans. Dielectr. Electr. Insul.* **1995**, *2*, 1.
-